Electronic Supplementary Information

Substrate-free and label-free electrocatalysis-assisted biosensor for sensitive detection of microRNA in lung cancer cells

Lin Cui[a] ‡, Meng Wang[a] ‡, Bing Sun[b] *, Shiyun Ai[c], Shaocong Wang[a], Chun-yang Zhang[a] *

[a] College of Chemistry, Chemical Engineering and Materials Science, Collaborative Innovation Center of Functionalized Probes for Chemical Imaging in Universities of Shandong, Key Laboratory of Molecular and Nano Probes, Ministry of Education, Shandong Provincial Key Laboratory of Clean Production of Fine Chemicals, Shandong Normal University, Jinan 250014, China

[b] School of Science, China University of Geosciences (Beijing), Beijing 100183, China

[c] College of Chemistry and Material Science, Shandong Agricultural University, Taian 271018, China

* Corresponding author. Tel.: +86 0531-86182538; Fax: +86 0531-82615258; E-mail: cyzhang@sdnu.edu.cn; Tel: +86-10-82322758; E-mail: sunbing@cugb.edu.cn

MATERIALS AND METHODS

Materials. Dicyandiamide, Tris (hydroxymethyl) aminomethane (Tris), gold chloride ($HAuCl_4$), thionine, tris(2-carboxyethyl)phosphine hydrochloride (TCEP) and 6-mercaptohexanol (MCH) were purchased from Sigma-Aldrich. Poly A polymerase was obtained from New England Biolabs (Ipswich, MA, USA). The RNase inhibitor and RNase-free water were obtained from TaKaRa Bio. Inc. (Dalian, China). Sodium acetate (NaAc), acetic acid (HAc) and H_2O_2 (30 wt%) were

purchased from Nanjing Chemical Reagent Co., Ltd. (Nanjing, China). Other reagents were of analytical grade and used as received. Ultrapure water obtained from a Millipore water purification system was used in all experiments. The synthetic oligonucleotides (**Table S1**) were purchased from Sangon Biological Engineering Technology & Services Co., Ltd. (Shanghai, China) and purified by high-performance liquid chromatography.

Table S1. Sequence of the Oligonucleotides

name	sequence (from 5' to 3')
capture probe	**CTC GGG GCA GCT CAG TAC AGG A**-SH
microRNA (microRNA-486-5p)	**UCC UGU ACU GAG CUG CCC CGA G**
single-base mismatched strand	UCC UGU ACU GAG CUG GCC CGA G
three-base mismatched strand	UCC UGG ACU GAG CUG GCC CGU G
T-rich assistant probe	TTT TTT TTT TTT TTT TTT TTT TTT TT

The binding regions in capture probe and microRNA are shown in bold. The mismatched bases in microRNA are shown in underline.

Apparatus and Characterization. The transmission electron microscopy (TEM) images were obtained on a Hitachi HT7700 transmission electron microscope (JEOL Ltd., Japan). The X-ray diffraction (XRD) analysis was performed on a diffractometer (X'Pert Pro Super, Philips) with Cu Kα radiation (λ = 1.54178 Å). Surface-enhanced Raman spectroscopy (SERS) spectra were measured by a LabRAM HR-800 (HORLBA JY, France) with an Ar ion laser (514.5 nm). The X-ray photoelectron spectroscopy (XPS) measurements were carried out on a spectrometer (MKII, ESCALAB) with Mg Kα as the excitation source. Cyclic voltammograms (CVs) and different

pulse voltammetry (DPV) measurements were performed on a CHI 660D electrochemical workstation (CHI, Shanghai, China) at room temperature using a conventional three-electrode system with a modified glassy carbon electrode (GCE) as the working electrode, a platinum wire as the auxiliary electrode, and a saturated calomel electrode as the reference electrode. Electrochemical impedance spectroscopic (EIS) analysis was performed with an Zahner workstation (Zahner, Elektrik IM6, German) in 0.1 M KCl containing 5 mM $[Fe(CN)_6]^{3-}$/$[Fe(CN)_6]^{4-}$ over a frequency range from 10 kHz to 0.1 Hz using an alternative voltage with an amplitude of 10 mV.

Synthesis of FeCN. Dicyandiamide (12 mmol) was mixed with iron (II) chloride hexahydrate ($FeCl_2 \cdot 6H_2O$, 0.84 mmol), and the homogeneous mixture was placed on a quartz boat and heated at 500 °C in a tube furnace for 2 h in Ar atmosphere to get the Fe^{2+}-g-C_3N_4. The temperature was further raised to 900 °C at a ramp of 10 °C/min and kept at 900 °C for 2 h in Ar atmosphere to obtain a black powdered material. After grounded into fine in the mortar, the obtained FeCN was restored in the desiccators.

Preparation of Electrochemical Biosensor. The electrochemical sensor was constructed on a GCE electrode. Prior to modification, the GCE electrode was polished with 1.0, 0.3, and 0.05 μm α-Al_2O_3 slurry, respectively, followed by successive sonication with pure water and ethanol for 3 min. The 10 μL of FeCN solution (1 mg mL^{-1}) was dropped onto the surface of GCE to obtain the FeCN/GCE. After drying at room temperature, 10 μL of AuNPs (13 nm diameter)[1] was dropped on the FeCN/GCE to obtain the AuNPs/FeCN/GCE. Meantime, the thiolated capture probe (0.5 μM) was activated by 50 μM TCEP for 1 h to reduce the disulfide-bonded oligonucleotides. After washing with pure water and drying in a nitrogen stream, 10 μL of 0.5 μM capture probes was

dropped on the electrode and incubated at room temperature over night. After rinsing with 10 mM Tris−HCl buffer (pH 7.4), 10 μL of 1 mM 6-mercaptohexanol (MCH) was dropped on the electrode for 30 min to block the unmodified sites.

Electrochemical detection of microRNA. The DNA-RNA hybridization was performed by incubating the capture probe/FeCN/GCE with 10 μL of target microRNA in hybridization buffer containing various concentrations of microRNA for 2 h at 37 °C. After rinsing with 10 mM Tris−HCl (pH 7.4) for three times, the electrode was incubated with a mixture of yeast poly A polymerase (10 U mL^{-1}) and 5 mM ATP in poly A polymerase extension solution (20 mM Tris−HCl, 50 mM KAc, 10 mM $Mg(Ac)_2$, 0.25 mM $CoCl_2$, pH 7.9) at 37 °C for 60 min, followed by rinsing with 10 mM Tris−HCl (pH 7.4) for three times. Then the modified electrode was exposed to 10 μL of the freshly prepared T-rich assistance probe (1 μM) to form the poly T/extended microRNA/MCH/capture probe/AuNPs/FeCN/GCE. After washing with 10 mM Tris−HCl, the 10 μL of 1 mg mL^{-1} thionine was dropped onto the above modified electrode, and incubated at 37 °C for 1 h. After rinsing with ultrapure water to remove the nonspecific adsorption thionines, the obtained biosensor was measured in HAc-NaAc solution (0.1 M, pH 5.0) to examine the DPV response.

Preparation of Cell Extracts. The lung adenocarcinoma cell line (A549 cells) were cultured in Dulbecco's modified Eagle's medium (DMEM, Life Technologies, USA) with 10% fetal bovine serum (FBS, Life Technologies, USA) and 1% penicillin–streptomycin at 37 °C with 5% CO_2. The total RNA was obtained by miRNeasy Mini Kit (Qiagen, German) according to the manufacturer's protocol and its concentration was determined by the NanoDrop 2000c spectrophotometer (Thermo Scientific, Wilmington, DE, USA).

SUPPLEMENTARY RESULTS

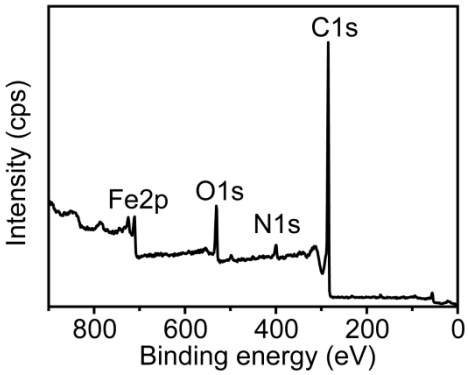

Fig. S1 XPS survey spectrum of the synthesized FeCN.

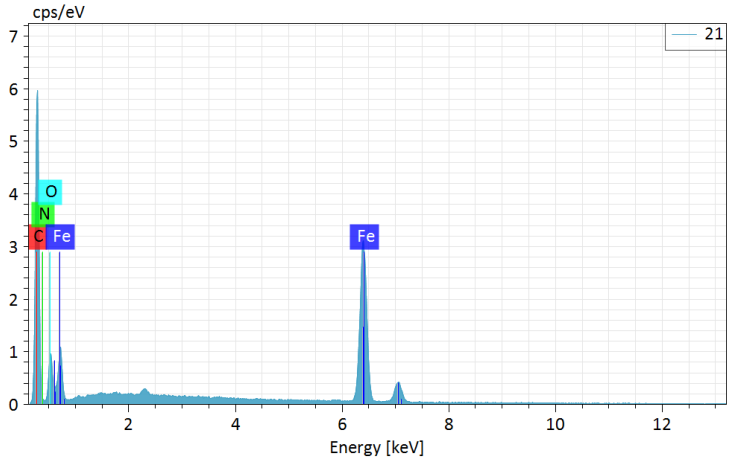

Fig. S2 Energy dispersive X-ray spectroscopy (EDX) indicates the existence of Fe, C, N and O in FeCN.

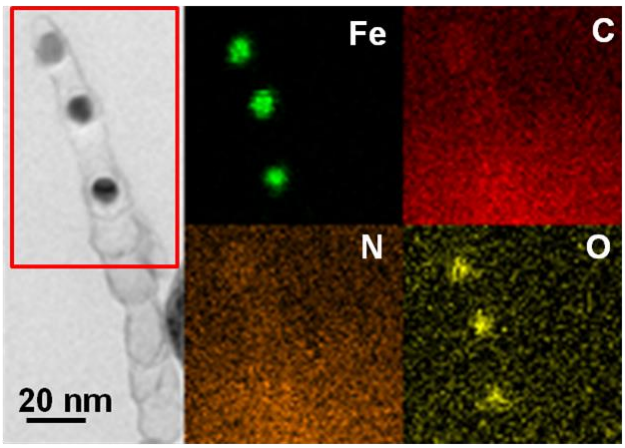

Fig. S3 TEM image of FeCN and the elemental mapping images of Fe, C, N, and O.

Effect of Varying Scan Rate. We recorded the cyclic voltammtric curves of thionines at either bare GCE or FeCN/GCE with different scan rate varying from 10 to 100 mV s^{-1} (Fig. S4). The CV anodic and cathodic peak currents enhance with the increasing scan rate from 10 to 100 mV s^{-1} (Fig. S4A and S4B). As shown in Fig. S4C, the anodic (black and blue curves) and cathodic peak currents (red and green curves) enhance linearly with the increasing square root of scan rates from 10 to 100 mV s^{-1}. The linear regression equations of thionines at the GCE are i_{pa} = 0.4135 $v^{1/2}$ + 0.9114 (R^2 = 0.9921) and i_{pc} = -0.1901 $v^{1/2}$ – 0.6470 (R^2 = 0.9886), while the linear regression equations of thionines at the FeCN/GCE are i_{pa} = 0.1682 $v^{1/2}$ - 0.1463 (R^2 = 0.9965) and i_{pc} = -0.1117 $v^{1/2}$ + 0.1483 (R^2 = 0.9957). The measured peak current is proportional to the square root of scanning rate ($v^{1/2}$), indicating the diffusion-controlled electrocatalytical reduction of thionines on the surface of the FeCN. The plot of i_{pc} vs $v^{1/2}$ obtained from the FeCN-modified GCE shows a steep slope compared with that obtained from the bare GCE, further verifying the catalytic role of FeCN in the electrochemical reduction of thionines.

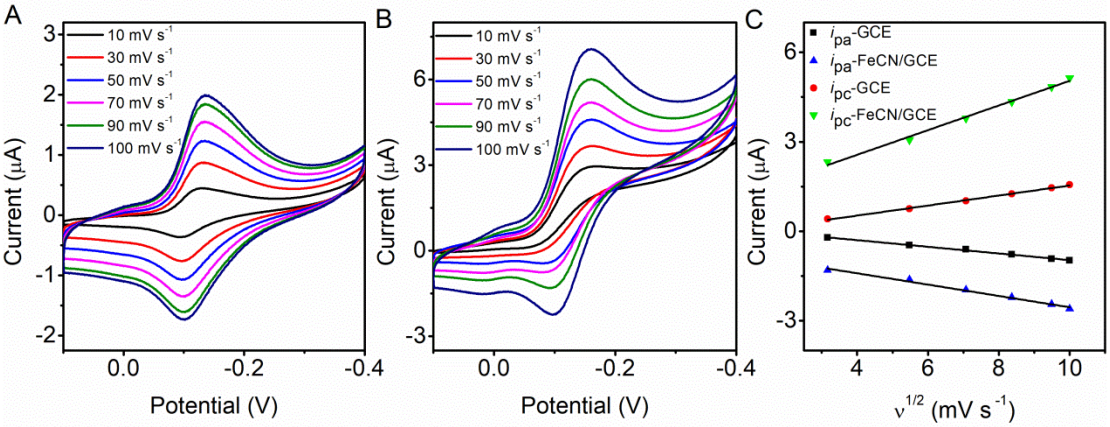

Fig. S4 CV curves of the bare GCE (A) and the FeCN/GCE (B) at different scan rates in 0.1 M HAc-NaAc solution (pH 5.0) containing 35 μM thionine. (C) Variance of i_{pc} and i_{pa} as a function of $v^{1/2}$ for the bare GCE (black and red curve) and the FeCN/GCE (blue and green curves) in 35 μM thionine at pH 5.0.

Electrochemical Characterization of Different Modified Electrodes. We investigated the stepwise fabrication process of the modified electrode and characterized the assembly of the sensing interface in 5 mM $[Fe(CN)_6]^{3-/4-}$ containing 0.1 M KCl. In comparison with the bare GCE (Fig. S5A, curve a), the modification of FeCN causes the increase of redox peak current (Fig. S5A, curve b) because FeCN can promote the electron transfer between $[Fe(CN)_6]^{3-/4-}$ and the electrode. When the AuNPs are electrodeposited onto the GCE, the redox current further increases (Fig. S5A, curve c) due to the good conductivity of AuNPs. After the capture probe and MCH are modified onto the sensing interface, the redox peak decreases (Fig. S5A, curve d) due to the electrostatic repulsion between $[Fe(CN)_6]^{3-/4-}$ and the negatively charged phosphate backbones of capture probe. The introduction of nonconductive MCH can block the nonspecific sites of sensing interface. Notably, a further decrease in redox peak is observed after the addition of target microRNA (Fig. S5A, curve e), the subsequent polyadenylation of the surface-bound microRNAs by poly(A) polymerase to form the poly(A) tails (Fig. S5A, curve f), and the formation of double-stranded DNAs (dsDNAs) through the hybridization of poly(A) tails with the T-rich assistance probes (Fig. S5A, curve g). This can be explained by the introduction of more negatively charged phosphate backbones onto the electrode surface.

The fabrication process of the biosensor is further verified by electrochemical impedance spectroscopy (Fig. S5B). When FeCN is coated onto the GCE, the R_{et} is decreased to 40.5 Ω (Fig. S5B, curve b) compared with the bare GCE (Fig. S5B, curve a) due to the good conductivity of FeCN. When the AuNPs are assembled onto the FeCN/GCE, the R_{et} is further decreased to 22 Ω (Fig. S5B, curve c). After assembling capture probes and MCH on the AuNPs/FeCN/GCE surface (Fig. S5B, curve d), an increased R_{et} (272 Ω) is observed because of the negatively charged phosphate backbone of DNA which attenuates the electron transfer. In addition, the short alkanethiol of MCH provides an insufficient barrier to block the electron transfer from the solution to the GCE. After the hybridization of target microRNA with the capture probe and the subsequent extension reaction induced by poly(A) polymerase, both the extended A-rich DNA sequences and T-rich assistant probes are immobilized on the GCE, the R_{et} values are increased to 1156 Ω and 1345Ω, respectively, because the negatively charged interface can electrostatically repel the

negatively charged redox probe $[Fe(CN)_6]^{3-/4-}$ and inhibits the interfacial charge transfer (Fig. S5B, curves e, f and g). These results suggest the successful fabrication of the electrochemical biosensor.

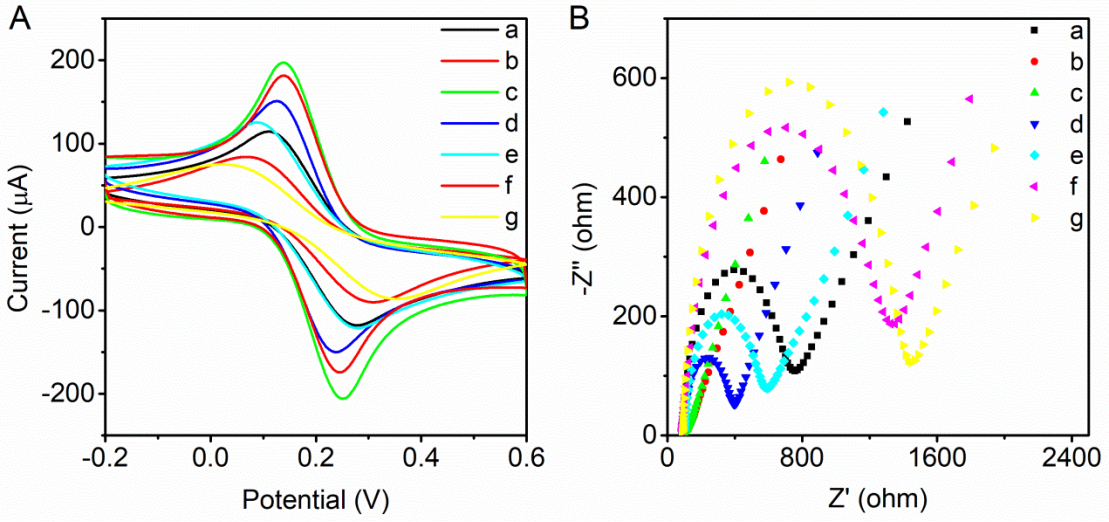

Fig. S5 CV (A) and EIS (B) characterization of different modified electrodes in 0.1 M KCl containing 5 mM $Fe(CN)_6^{3-/4-}$ in the range from 0.1 Hz to 10^5 Hz at an alternate voltage of 5 mV. (a) GCE, (b) the FeCN/GCE, (c) the AuNPs/FeCN/GCE, (d) the MCH/capture probe/AuNPs/FeCN/GCE, (e) the microRNA/MCH/capture probe/AuNPs/FeCN/GCE, (f) the extended microRNA/MCH/capture probe/AuNPs/FeCN/GCE, and (g) the T-rich assistant probe/extended microRNA/MCH/capture probe/AuNPs/FeCN/GCE.

Optimization of Experimental Conditions. To achieve the best assay performance, we optimized the experimental conditions including the concentrations of capture probe and poly(A) polymerase, the reaction time of microRNA-capture probe hybridization, and the reaction time of poly(A) polymerase-mediated single-stranded extension (Fig. S6). As shown in Fig. S6A, the electrochemical DPV response enhances with the increasing concentration of capture probe from 0.05 to 0.5 μM, followed by the decrease beyond the concentration of 2 μM. Thus, 0.5 μM capture probe is used in subsequent research. The effect of incubation time of microRNA-capture probe hybridization upon the assay performance is investigated as well (Fig. S6B). With the increase of incubation time from 20 to 120 min, the DPV responses enhances greatly and reaches a maximum value at 120 min. Thus, 120 min is selected as the optimal hybridization time in the subsequent research. Fig. S6C shows the effect of the concentration of poly(A) polymerase upon the assay performance. The current response improves with the increasing concentration of poly(A) polymerase and reaches a plateau at the concentration of 10 U mL^{-1}. Thus, 10 U mL^{-1} poly(A) polymerase is used in the subsequent research. We further investigated the influence of the incubation time of poly(A) polymerase upon the assay performance (Fig. S6D). The current response enhances with the incubation time rapidly and reaches the maximum value at 60 min. Thus, 60 min is selected as the optimal incubation time in the subsequent research.

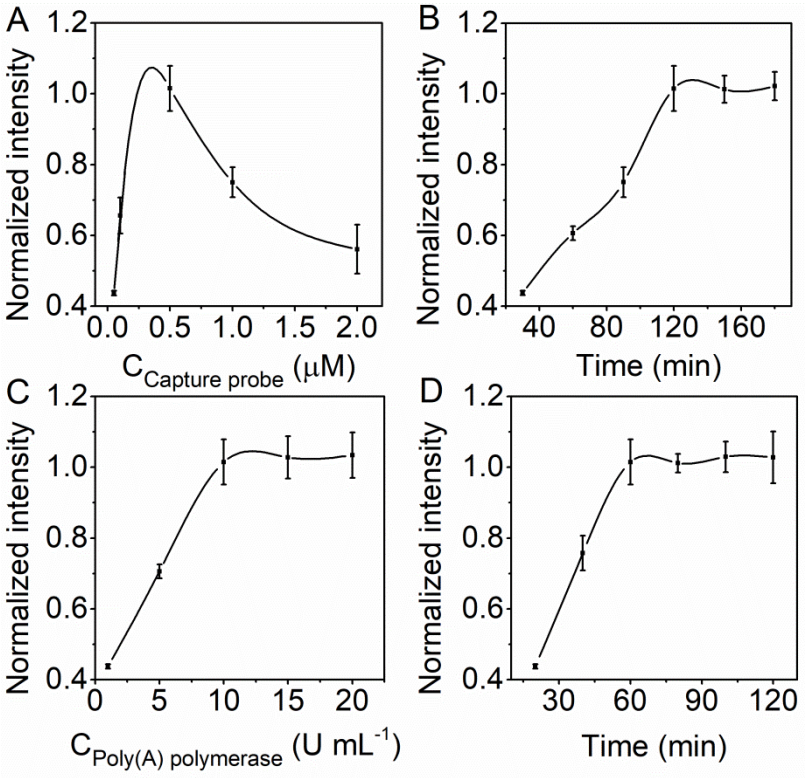

Fig. S6 Optimization of the capture probe concentration (A), the microRNA-DNA hybridization time (B), the poly(A) polymerase concentration (C), and the reaction time of poly(A) polymerase-mediated single-stranded extension (D). The microRNA concentration is 100 pM. Error bars represent the standard deviations of three experiments

Stability and Repeatability of Electrochemical Biosensor. The intra-assay precision of the obtained biosensor was evaluated by measuring 100 pM target microRNA with five different batches of biosensors under identical conditions. The intra-assay variation coefficient is 3.8%, demonstrating the good repeatability. The successive cyclic voltammograms (CV) scans were used to investigate the stability of the obtained biosensor. After 20 times of CV scans, 96% of the initial response of the electrochemical biosensor can still be detected (Figure S7). In addition, the obtained biosensor was stored at 4 °C and measured every 4 days to monitor the stability. The electrochemical signal of the biosensor can still maintain 92.3% of the original response after 20 days, demonstrating long-term stability of the obtained biosensor.

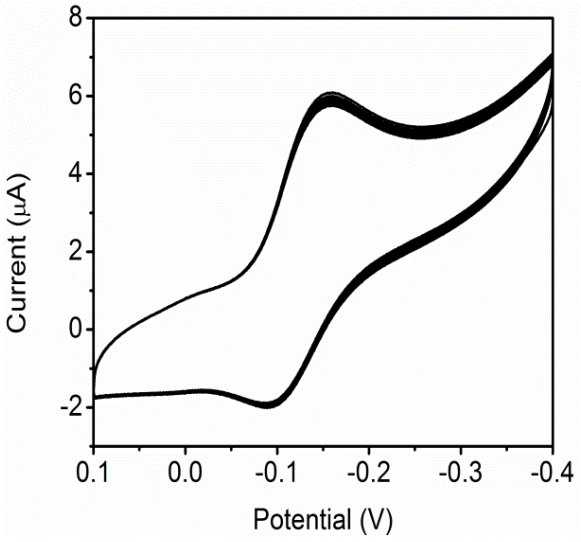

Fig. S7 Stability and Repeatability of the obtained biosensor for the detection of 100 pM microRNA after 20 times of CV scans.

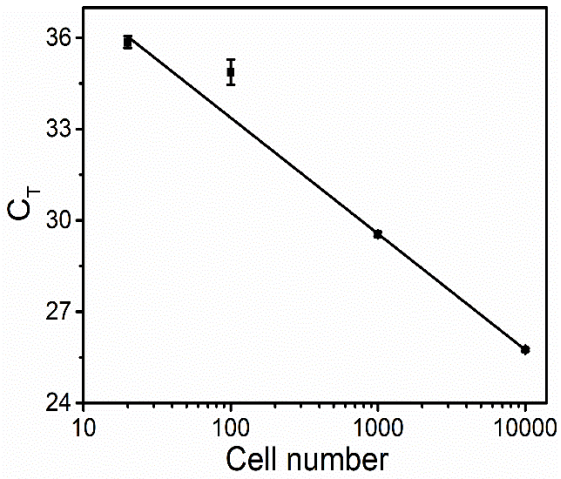

Fig. S8 Linear correlation between C_T and the logarithm of A549 cell number in the range from 20 to 10000 cells. Error bars represent the standard deviations of three independent experiments.

Table S2. Comparison of Different Methods for Label-Free Detection of MicroRNA

detection method	linear range	detection limit	cell analysis	ref.
fluorescence	0.05 μM - 2.5 μM	50 nM	Yes	2
fluorescence	10 pM - 400 pM	10 pM	No	3
fluorescence	0.1 pM - 10 nM	0.18 pM	Yes	4
fluorescence	100 fM - 1.0 pM	33.4 fM	NA	5
fluorescence	100 fM - 10 nM	12.8 fM	Yes	6
colorimetry	20 pM - 10 nM	20 pM	Yes	7
colorimetry	10 fM- 10 nM	7.4 fM	Yes	8
electrochemistry	1.0 pM - 10.0 nM	0.26 pM	No	9
electrochemistry	0.1 pM - 10 pM	45 fM	No	10
electrochemistry	10 fM - 1 pM	12 fM	Yes	11
electrochemistry	10 fM – 1000 fM	1.7 fM	No	12
electrochemistry	1 fM - 1000 pM	0.853 fM	Yes	this work

References

1. A. Ambrosi, M. T. Castañeda, A. J. Killard, M. R. Smyth, S. Alegret and A. Merkoçi, *Anal. Chem.*, 2007, **79**, 5232-5240.
2. J. Zhang, L. Chao, Z. Xiao, G. A. Ramón, Y. Liu, C. Zhang, P. Fei and D. Cui, *Anal. Chem.*, 2015, **88**, 1294–1302.
3. F. Xu, H. Shi, X. He, K. Wang, D. He, Q. Guo, Z. Qing, L. Yan, X. Ye and D. Li, *Anal. Chem.*, 2014, **86**, 6976-6982.
4. L. R. Zhang, G. Zhu and C. Y. Zhang, *Anal. Chem.*, 2014, **86**, 6703-6709.
5. X. Miao, Z. Cheng, H. Ma, Z. Li, N. Xue and P. Wang, *Anal. Chem.*, 2017, **90**, 1098-1103.
6. F. Ma, M. Liu, B. Tang and C. Y. Zhang, *Anal. Chem.*, 2017, **89**, 6182–6187.
7. T. Tian, H. Xiao, Z. Zhang, Y. Long, S. Peng, S. Wang, X. Zhou, S. Liu and X. Zhou, *Chem.–Eur. J.*, 2013, **19**, 92-95.
8. H. Wu, Y. Liu, H. Wang, J. Wu, F. Zhu and P. Zou, *Biosens. Bioelectron.*, 2016, **81**, 303-308.
9. D. Zhu, W. Liu, D. Zhao, Q. Hao, J. Li, J. Huang, J. Shi, J. Chao, S. Su and L. Wang, *ACS Appl. Mater. Interfaces*, 2017, **9**, 35597–35603.
10. N. Xia, L. Zhang, G. Wang, Q. Feng and L. Liu, *Biosens. Bioelectron.*, 2013, **47**, 461-466.
11. Q. Tian, Y. Wang, R. Deng, L. Lin, Y. Liu and J. Li, *Nanoscale*, 2015, **7**, 987-993.
12. Y. Zhou, H. Yin, J. Li, B. Li, X. Li, S. Ai and X. Zhang, *Biosens. Bioelectron.*, 2016, **79**, 79-85.